International Journal of Innovative Technology and Exploring Engineering (IJITEE)
ISSN: 2278-3075 (Online), Volume-9 Issue-2, December 2019

Innovative and Efficient Electric Braking System In High-Speed Trains using Proportional Resonant Controller

Saranu Ravikumar

Abstract*: The high-speed trains are eight times more efficient than traditional trains because it significantly operates faster than the other trains; however, the train accidents are happened as because of its poor braking system. From this reason, effective braking system control techniques are developed. In this paper, the electric brake regenerative system is introduced to control the high-speed train. Therefore the braking system of a high-speed train is modeled in Brushless Direct Current (BLDC) motor, which is controlled by the gain of Proportional Resonant (PR) controller. Subsequently, the parameters of the controller and error percentage from the controller in the braking system are optimized using Multi-Objective African Buffalo Optimization (MOABO). The developed controller in braking system stability is analyzing by the Lyapunov function. The results of the braking system are validating by the torque and speed of the high-speed train braking system. Furthermore, the proposed high-speed braking system control is compared with existing control techniques in a high-speed train.

Keywords* : Braking system, Brushless Direct Current motor, Current controller, Stability analysis.

I. INTRODUCTION

In recent times, the high-speed train plays a considerable role in encouraging the growth of the industrial fasten and the latest industrial services in the city, as well as the raise of the inhabitants stream rate and the inhabitants addition in the regions along the strap and road in many countries [1]. Nevertheless, the safety measures are considered as a very important section in the high-speed train. Because the faults in train braking system tend to causes an accident with a huge loss [2]. Thus the braking system in high-speed trains plays an essential role to avoid accidents [3]. Formerly, the brake pad materials are often used in high-speed trains, which is formed by Copper (Cu) - based composite materials [4]. Moreover, the production of metal matrix friction can be separated into powder metallurgy and monomer metal casting materials such as cast iron, steel, bronze, etc. [5]. Nevertheless, the powder metallurgy and monomer metal casting had been eliminated as because of its restriction in braking systems [6], [7].

Revised Manuscript Received on December 30, 2019.
***** Correspondence Author
Saranu Ravikumar*, Assistant Professor, Department of Mechanical Engineering, Bapatla Engineering College, Bapatla-522102, Andhra Pradesh, India. Email: ravikumar.saranu@gmail.com

Besides, there are six types of braking systems are used in high-speed train [8] namely mechanical braking scheme, hydraulic braking system, pneumatic or air braking system, vacuum braking method, magnetic braking coordination and electric braking system. Furthermore, in prior times, the stress of rails has dramatically increased due to the reason of high-speed and overloaded trains [9]; therefore the identification of damage part in track is the critical case [10]. To resolve these issues by the eddy current brake based scheme with optimization approach is introduced [11]. The performance of braking system in high-speed train is enhancing by the eddy current brake [12], which is also known as an electric brake or induction brake [13]. Consequently, the eddy current brake system is a more effective and highly applicable method in the braking system of high-speed trains [14]. To guarantee secure operations braking scheme of high-speed trains is essential to keep massive braking forces in control [15].

In recent literature, the performance of the braking system is defining by the friction materials. However, there is a complexity occurs in friction material. From this reason, Serrano-Munoz *et al* [16] proposed a sintered friction material for the obscure mechanism of the braking system. Moreover, the thermocouples are placed in the system to monitor the friction material temperature and the real-scale dynamometer is used to the braking program. In a high-speed train, the high running speed and heavy carrying capacity is the necessary goal. Hence Peng Zhang *et al* [17] proposed the brake pads based on the copper with Aluminum Oxide (Al_2O_3) fiber for the high-speed and larger load of the train breaking performance improvement. Moreover, with and without fibers are tested in two fabricated tests on a reduced-scale dynamometer is taken by this approach. Consequently, the friction coefficient raised and stabilized the coefficients at the heavy load and high running speed. The coefficient of friction based layer is the key to safety measures, thus the friction coefficient is a major mechanism in the braking pads to ensure the safety of the high-speed trains. Hence, Peng Zhang *et al* [18] proposed brake pads based on the copper for the endangered braking conditions. Moreover, here explained the friction coefficient losses based on the changes in the friction layer. To enhance the braking system with ceramic procedure, Yelong Xiao *et al* [19] proposed Copper Metal Matrix Composite (Cu-MMC) for the brake pads in the high-speed trains. Moreover, it is a powder metallurgy method based braking system.

The full-scale dynamometer is used to estimate the properties of mechanical and microstructure of the Cu-MMC and the performance of the braking enhanced under the dynamic braking conditions. In past decades, controlling the friction and characteristics of wear material in the high-speed railways braking system is the major challenge. Hence, Peng Zhang *et al* [20] proposed copper-based brake plates containing Iron powders for the friction coefficient stabilization. The properties of friction and wear of the braking pad materials are tested effectively in the high-speed railways. Nevertheless, the mechanical braking scheme usage in the high-speed train has some severe difficulties as because of its wastage of kinetic energy, this leads to the poor performance of the system. To address those problems, in this current research a new regenerative electric braking system is designed to control the high-speed train braking.

The key contribution of this research is initially the train brake pedaling system with the use of Brushless DC motor is designing. Afterward, the current constraint in the BLDC motor is regulated using PR controller. Consequently, the parameter of the PR controller is optimized using ABO approach. Moreover, the stability of the PR controller is analyzed using Lyapunov function. Therefore, the proposed braking strategies enhance the efficiency of the braking system. The rest of this work is organized as, Section 2 elaborated the model of high-speed train system and Electric braking system with BLDC motor, Section 3 detailed about the proposed control strategies and optimization, section 4 described the result and discussion, comparison with existing techniques, finally section 5 concludes the paper.

II. MATHEMATICAL MODEL OF HIGH-SPEED TRAIN TRACTION MOTOR

The dynamic model of high-speed train can be expressed by the subsequent (1) as,

$$m'_j v'_j = u'_j + f'_{j-1} - f'_i - \hat{F}_j^R, \quad j = 1,2,...n \tag{1}$$

$$\hat{F}_j^R = \hat{M}_j^R + \hat{L}_j^R + \hat{C}_j^R \tag{2}$$

Where the mass of the j^{th} block is termed as m'_j, braking or traction efforts of j^{th} block is u'_j, the force of the coupler j^{th} block is denoted as f_i' and $\hat{F}_j^R$ is represents as the normal running resistance created on the j^{th} block, $\hat{L}_j^R$ is the resistance of track gradient, $\hat{C}_j^R$ is the resistance of line curvature and $\hat{M}_j^R$ is the resistance of rolling in (2). Besides the high-speed trains are running with the help of electric motors terms as Brushless DC motor Fig. 1. Moreover in BLDC motor, the coils are not placed on the rotor and permanent magnet is fixed instead of the rotor [21]. However, the coils are not rotated also it is fixed in stator place. As because of the coils are stable in brushless motor, so there is no need of brushes and commutator. The permanent magnet is rotated in BLDC motor. Rotation is attained by altering the track of the magnetic fields, which is produced by surrounding motionless coils. The rotation is controlled by adjusting the magnitude and its direction. The torque measure T_m can be defined in (3), the angular motion of BLDC motor is elaborated in (4) and the relation among angular position and angular velocity in (5).

$$T_m = h_a(\theta_s) i_a + h_b(\theta_s) i_b + h_c(\theta_s) i_c / \omega \tag{3}$$

$$T_m = M \frac{d\omega_e}{dt} + \hat{T}_L + D\omega_e \tag{4}$$

$$\frac{d\theta_s}{dt} = \frac{l}{2}\omega_e \tag{5}$$

Where, T_m is the torque measured, back emf of motor in volts is h_a, θ_s is the state variable, the input current of motor is (i_a, i_b, i_c), M is the inertia of rotor $[kgm^2]$, D is the damping constant, $\hat{T}_L$ is the torque load $[N-m]$, l is the count of rotor poles, B is denoted as friction coefficient and M as inaction of the motor. Moreover, the friction coefficient is neglecting from the (4), then the torque is represented in the braking system is in (6) as,

$$T_m = M \frac{d\omega_e}{dt} \tag{6}$$

Even though at the time of braking condition the measured torque T_m tends to negative, then it is portrayed as $T_m = -\tilde{K}_t i_a$. Afterwards the braking torque is expressed in (7) as,

$$M \frac{d\omega_e}{dt} = -\tilde{K}_t i_a \tag{7}$$

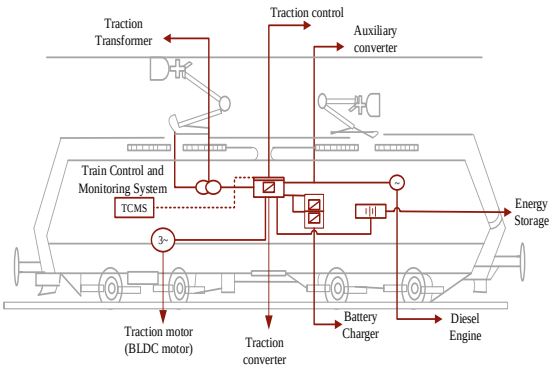

Fig. 1.The schematic diagram of dynamic model of high-speed train system

III. CONTROLLER DESIGN IN BRAKING SYSTEM

The flux and torque estimator unit measure the torque of the electric machine and flux of stator from the current and terminal voltage measurements. The estimated flux of stator and torque are regulated straightly by contrasting them with its relevant required values. The schematic diagram of the speed control in high-speed train braking system is shown in Fig. 2. The reference flux and torque utilized in the PR controller presented by the speed controller of high-speed train.

A. PR Controller

Once the orientations of negative and positive sequence currents are dogged, it is difficult to control both negative and positive components in $\alpha\beta$ stationary frame accurately. The development of PR controller in BLDC motor is to control the braking system of high-speed train. Besides, it controls the overall current including both negative and positive components. The calculated Direct Current (DC) fed into the regulator which has pedestal however, the reference signals are separated in the form of negative and positive rotating synchronous edge. The block diagram of the PR controller is shown in Fig. 3. Moreover, the process of current regulator based on open-loop transfer utility can be elaborated in (8).

$$C(s) = R_{ip} + \frac{sR_{iI}}{s^2+\omega_p^2} + \frac{sR_{iI}}{s^2+(3\omega_p)^2} + \frac{sR_{iI}}{s^2+(5\omega)^2} \tag{8}$$

The coefficient of proportional and resonant can be defined as R_{ip} and R_{iI}, $\omega_p = 2\pi f$, the line frequency $f = 50$ Hz. PR controller is introduced to measure the random performance of the system under exterior turbulence and the large gain of the fundamental frequency is achieved. The planned control format is recognized in a single fixed orientation frame to compensate both negative and positive series components under unbalanced circumstances. As a significance, the computational load is noticeably reduced when it judges against other conventional controllers.

The transformation process from dq synchronous base frame to $\alpha\beta$ reference frame set is evaluated using (9).

$$G_{\alpha\beta}(T) = \frac{1}{2}\begin{bmatrix} G_{dq}^{+} + G_{dq}^{-} & JG_{dq}^{+} - JG_{dq}^{-} \\ JG_{dq}^{+} + JG_{dq}^{-} & G_{dq}^{+} - G_{dq}^{-} \end{bmatrix} \tag{9}$$

$$G_{dq}^{+} = G_{\alpha\beta}(T + J\omega) \tag{10}$$

$$G_{dq}^{-} = G_{\alpha\beta}(T - J\omega) \tag{11}$$

Where, $G_{\alpha\beta}$ is the base reference frame. Furthermore, the equivalent control transfer function for the positive sequence element, while $G_{dq}(T) = \frac{R_i}{T}$ is defined in (12).

$$G_{\alpha\beta}^{+} = \frac{1}{2}\begin{bmatrix} \frac{2R_{ri}t}{t^2+\omega_r^2} & \frac{2R_{ri}\omega}{t^2+\omega_r^2} \\ -\frac{2R_{ri}\omega}{t^2+\omega_r^2} & \frac{2R_{ri}t}{t^2+\omega_r^2} \end{bmatrix} \tag{12}$$

Where R_{ri} is the resonant gain, ω_r is the integral resonant frequency. Consequently, the equivalent control transfer function for the negative sequence element, while $G_{dq}(T) = \frac{R_i}{T}$ is defined in (13).

$$G_{\alpha\beta}^{-} = \frac{1}{2}\begin{bmatrix} \frac{2R_{ri}t}{t^2+\omega_r^2} & -\frac{2R_{ri}\omega}{t^2+\omega_r^2} \\ \frac{2R_{ri}\omega}{t^2+\omega_r^2} & \frac{2R_{ri}t}{t^2+\omega_r^2} \end{bmatrix} \tag{13}$$

From the derivations the diagonal elements of both (12) and (13) are equal. However, the opposite direction of diagonal elements indicates the reverse direction of negative and positive component, which is elaborated using (14).

$$G_{\alpha\beta}(T) = G_{\beta\beta}^{+}(T) + G_{\alpha\beta}^{-} \tag{14}$$

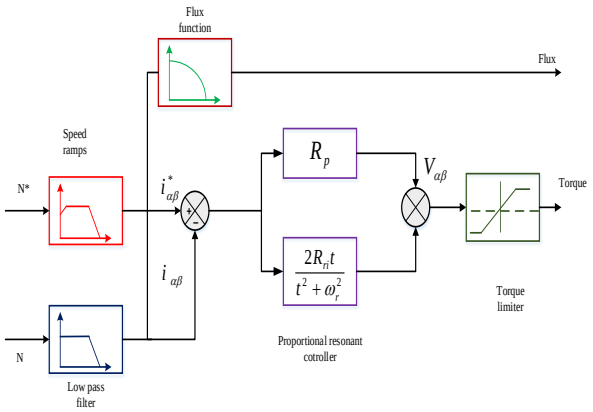

Fig. 2.Speed control of high-speed train braking system

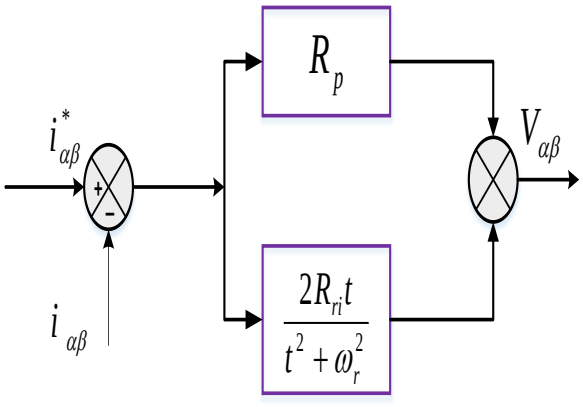

Fig. 3.PR controller block diagram

$$G_{\alpha\beta}(T)=\frac{1}{2}\begin{bmatrix}\frac{2R_{ri}t}{t^2+\omega_r^2} & 0\\ 0 & \frac{2R_{ri}t}{t^2+\omega_r^2}\end{bmatrix} \quad (15)$$

Zero indicates off-diagonal elements of a transfer function in (15), the cross pairing among alpha and beta signals on fixed reference bloc is negated. Moreover, the compensation of voltage feed is also eradicated. Furthermore, in the unbalanced condition the burden voltage has sinusoidal capacities of both negative series components and positive series components in the solitary motionless reference frame. Therefore the PR controller with right tuning is proficient to control both the negative and positive sequence currents concurrently in the static reference frame. The transfer function of PR controller is defined in (16).

$$G_{\alpha\beta}(T)=R_p+\frac{2R_{ri}t}{t^2+\omega_r^2} \quad (16)$$

Where the proportional gain is denoted as R_p, resonant gain as R_{ri} and the resonant frequency is denoted a ω_r. Moreover, the PR controller in BLDC motor for high-speed train braking can achieve high gain which is close to frequency resonant therefore the proficient to eliminate the steady state fatal flaw between the reference and restrained control signal. The dynamic enactment of the controller is dogged with the right tuning of its controller factors. The parameters are attuned by function the frequency reply analysis. The characteristics of magnitude are plotted by $R_p=1$ also the gain of integral resonant as $\omega_r=314 rad/s$. The bandwidth is based on gain integral of the resonant series. Moreover, the huge value of resonant gain tends to broader bandwidth and minor value results in tapered bandwidth. Thus the voltage base signal $V_{\alpha\beta}$ is elaborated using (17).

$$V_{\alpha\beta}=\left(R_p+\frac{2R_{ri}t}{t^2+\omega_r^2}\right)(i^*_{\alpha\beta}-i_{\alpha\beta}) \quad (17)$$

B. MOABO Algorithm

ABO attempts to unravel the problem of pre-mature stagnation or convergence by guarantees the location of each buffalo, moreover the location of each buffalo is regularly updated. In relative to the particular buffalo's the best preceding location and the current location of the best buffalo in the drove. The model of ABO has three important characteristics behavior which is extensive intelligence capacity, cooperative in nature and democratic nature. In addition the learning parameters such as exploration and exploitation can help for the movement of the buffalo's. The flow of work process is elaborated in Fig. 4.

In the exploitation is used to find a safer location and exploration is for searching food. Moreover, the communication of the buffalo's is studied under "waaa" and "maaa" sounds. Thus the ABO calculation arbitrarily initializing in (18) the buffalo to location into the search space, it evaluates the exploitation and exploitation fitness respectively using (19) to each buffalo to determine the herd's best animal as well as individual buffalo personal best location $(bu.k^*)$.

$$p^*k^*=p^*k^*+lu1(bg-w_k^*)+lu2(bu.k^*-w_k^*) \quad (18)$$

$$w^*k^{*1}=\frac{w_{k^*}^*+m^*k^*}{\lambda^*} \quad (19)$$

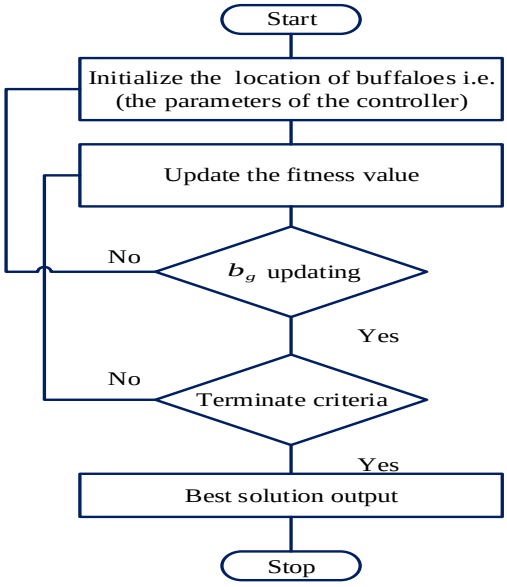

Fig. 4.The flow chart of MABO for PR controller parameter tuning

Where w_k and p_k represent the respective exploration and exploitation fitness of $k^*(k^*=1,2,3....N)$, $lp1$, $lp2$ are the learning parameters bg denotes the best location of each buffalo λ denotes the random number. Moreover the probability of buffalo can be calculated by the (20) as,

$$P_{ab^*}=\sum_{ab=1}^{s}\frac{w^{lp1}ab^*p^{lp2}ab^*}{w^{lp1}ab^*p^{lp2}ab^*} \quad (20)$$

Where p is the symbol of the "maaa" sound of the buffalo, w is the symbol of the "waaa" sound of the buffalo and ab^* is the buffalo move the explore curve.

Consequently, the probability of buffalo d is leaving from the vertex of a and b. In this research the multi-objective ABO algorithm is used to tuning and optimizing the constraints of PR controller for high-speed train braking system.

C. Stability Analysis

The stability evaluation of the controller is more important to evaluate how it remains stable while performing its dynamic condition. Thus the stability verification of PR controller is braking system is analyze using Lyapunov strategy [22]. However, the success of the controller function depends upon the stability measure. To evaluate the stability measure in PR controller using Lyapunov function following parameters should be satisfied such as L_1 and L_2, also the function of Lyapunov function is elaborated as f_1 and f_2. The positive terminal of Lyapunov function [23] can be elaborated in (21) also the process function of Lyapunov scheme is defined in (22) and (23).

$$f_1 = \frac{1}{2} r_1^2 \tag{21}$$

$$f_2 = f_1 + \frac{1}{2} r_2^2 + \sum_{i=1}^{l} \frac{1}{2} \Gamma_{b1}^{-1} \tilde{b}_i^2 + \frac{1}{2} \Gamma_{c0}^{-1} \tilde{c}_0^2 + \frac{1}{2} \Gamma_{d0}^{-1} \tilde{d}_0^2 + \sum_{i=1}^{l} \frac{1}{2} \Gamma_{n_i}^{-1} n_i \tilde{\rho}_i^2 \tag{22}$$

Where the positive constants are represented as Γ_{b1}, Γ_{c0}, Γ_{d0} and Γ_{ni} also $\tilde{b}_i = b_i - \hat{b}_i(t)$, $c_0 = c_i - \hat{c}_0(t)$, $\hat{d}_0 = d_0 - \hat{d}_0(t)$ and $\tilde{\rho}_i = \rho_i - \hat{\rho}_i(t)$ with $\hat{b}_i(t)$, $\hat{c}_0(t)$, $\hat{d}_0(t)$, $\hat{\rho}_i(t)$ are the inference of b_i, c_0, d_0 as well as $\rho_i = \frac{1}{n_i}$, respectively.

$$f_2 = f_1 + \frac{1}{2} r_2^2 + \sum_{i=1}^{l} \frac{1}{2} \frac{n_i}{\Gamma_{Lf}} \tilde{\rho}_{Lf}^2 + \sum_{i=1}^{l} \frac{n_i}{2} \Gamma_{\xi}^{-1} \xi^T \xi + \sum_{i=1}^{l} \frac{1}{2} \Gamma_{bi}^{-1} \tilde{b}_i^2 + \frac{1}{2} \Gamma_{c0}^{-1} \tilde{c}_0^2 + \frac{1}{2\Gamma_{d0}} \tilde{d}_0^2 + \sum_{i=1}^{l} \frac{1}{2} \Gamma_{n_i}^{-1} n_i \tilde{\rho}_i^2 \tag{23}$$

where, Γ_{Lf}, Γ_{ξ}, Γ_{bi}, Γ_{c_0} and Γ_{d_0} are the constants which remains positive, $\tilde{b}_i = b_i - \hat{b}_i(t)$, $\tilde{c}_0 = c_0 - \hat{c}_0(t)$, $\tilde{d}_0 = d_0 - \hat{d}_0(t)$, $\tilde{\rho}_{Lf} = \rho_{Lf} - \hat{\rho}_{Lf}$, $\tilde{\rho}_i = \rho_i - \hat{\rho}_i$, and $\tilde{\xi} = \xi - \xi(t)$ with $\hat{b}_i(t)$, $\hat{c}_0(t)$, $\hat{d}_0(t)$, $\tilde{\rho}_{Lf}$, $\hat{\rho}_i$, and $\xi(t)$. Moreover the functions of Lyapunov f_2 is calculated using (24) that contains $\tilde{\xi}$ and $\tilde{\rho}_{Lf}$. Thus the parameters of Lyapunov function represented as L_1 and L_2, which is defined in (24) and (25).

$$L_1 > \sum_{k=1}^{n} \left(\delta_{1,k} p_k^2 \rho_k^2 + \delta_{2,k} q_k^2 \rho_{2k}^2 \right) \tag{24}$$

$$L_2 > \sum_{k=1}^{n} \left(\delta_{1,k} p_k^2 \rho_k^2 + \delta_{2,k} q_k^2 \rho_{2k}^2 \right) \tag{25}$$

Therefore the function of Lyapunov process is defined in (26) as,

$$f'_2 = -L_1 r_1^2(t) - L_2 r_2^2(t) + C \tag{26}$$

Where, the condition of Lyapunov process is satisfied under the positive constants of L_1 and L_2 is expressed as in the (27) and (28) as,

$$L_1 = L_1 - \sum_{k=1}^{n} \left(\delta_{1,k} p_k^2 \rho_k^2 + \delta_{2,k} q_k^2 \rho_{2k}^2 \right) > 0 \tag{27}$$

$$L_2 = L_2 - \sum_{k=1}^{n} \left(\delta_{1,k} p_k^2 \rho_k^2 + \delta_{2,k} q_k^2 \rho_{2k}^2 \right) > 0 \tag{28}$$

Nevertheless, if the positive constants are true then f_2' is negative for some exterior case. The result should have the closed loop scheme that is equally enclosed with the states of $r_1(0)$ and $r_2(0)$. Recollect the values of $r_1(t)$ and $r_2(t)$ this result can conclude the stability analysis of PR controller in braking system under different operating conditions.

IV. RESULT AND DISCUSSION

Controlling and calculating the wear characteristics and friction of entrant materials for brake pads in high-speed trains is a challenging task and requires a simulative test process. The working of the proposed braking strategy is verified using simulation results. The implantation of the high-speed train braking system is performed on the simulation model MATLAB/Simulink R2018b, running on windows 10 platform. The brake pedal for the simulation is realized by ramp signal with various lopes and different voltage levels. Besides the BLDC motor rotor is designed by permanent magnet also the selection of magnetic material is confirmed by the density of the magnetic field. Moreover, the commutation in BLDC motor is controlled electronically; predominantly the stator windings in the motor should be energized in series to rotate the motor.

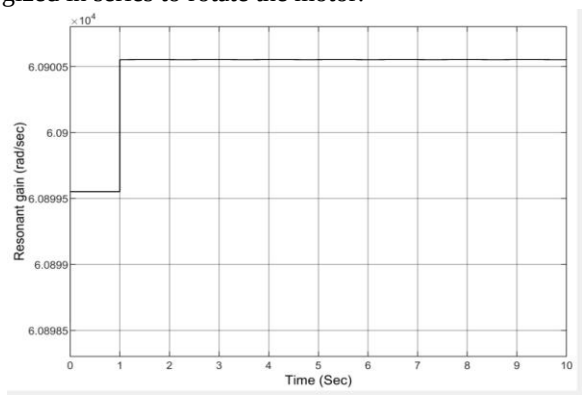

Fig. 5.The resonant gain of PR controller in the braking system

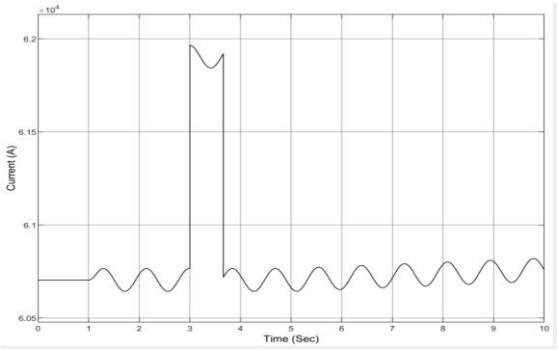

Fig. 6.The output waveform of the motor current

Furthermore, the parameter of torque measure elaborates the performance of BLDC motor, torque parameters of BLDC motor such as rated torque and peak torque. The braking system of the high-speed train is performed by the gain of the PR controller and the controller gain tuning as well optimizing by multi-objective ABO optimizer. From this reason, when the current is controlled efficiently then the friction has happened and it stops the train.

The small resonant gain in PR controller deals with very high gain in a tapered frequency band, which is close to the resonant frequency to track the current signals to diminish the steady-state fatal flaw between calculated and orientation signal and ensures the better dynamic reply of the controller. The average gain of proportional resonant controller is 314 rad/sec. Consequently, the proposed MOABO tuned the PR controller resonant gain and optimized as 419 rad /sec in Fig. 5. The rise time of the proposed controller is 0.067 seconds and the settling time of the controller is attained in the range of 1 second, nevertheless, there is no overshoot occurred in the controller.

The output waveform of the BLDC motor in the train is shown in Fig. 6. At the initial stage, the current of the motor is gradually raised, once the speed of the train attained stable value then the current drops down.

The brake commands and acceleration are specified to the control component that impels the motor for different driving conditions. When acceleration rule has pertained, the brake domination is inactive respectively. The pedaling or switching time of braking pads is shown in Fig. 7.

The measured torque characteristic of the high-speed train motor is shown in Fig. 8. Primarily the torque of the motor attained stable range then the torque minimized to the rated range. Moreover, at the instant $t = 0.5$ sec the load torque is raised to twice the range. Therefore the measured torque also raised by the equivalent percentage.

The Output graphic representation of the speed of the motor in a train is shown in Fig. 9. The set response of the motor speed is 12000 rpm; the motor attained the set speed rapidly with the use of PR and MABO control. At this point, the load torque is minimizing from 0.24 to 0.1 Nm at time 0.5 sec. After that the speed of the BLDC motor increase. Thus traction motor also works at corresponding currents and different speed levels, and the association among current and torque determined the torque values. Subsequently, the association among speed and torque can be interpolated with the torque-speed linear condition in BLDC motor.

Furthermore, the efficiency of proposed techniques used in the high-speed train braking system is compared with existing techniques like Adaptive Controller (AC) [25] and Cooperative Cruise Control (CCC) [26] are elaborated as follows. The gain achieved by the proposed PR controller is 6.07 rad/sec at the parameter point of R_{ri} is 1 and ω_r as 0.127.

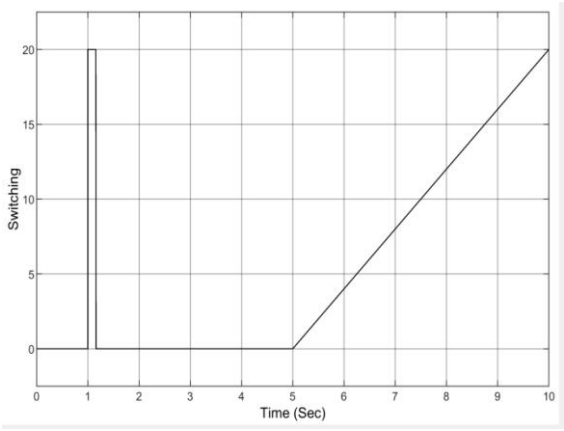

Fig. 7.Pedaling time of braking pads in the high-speed train

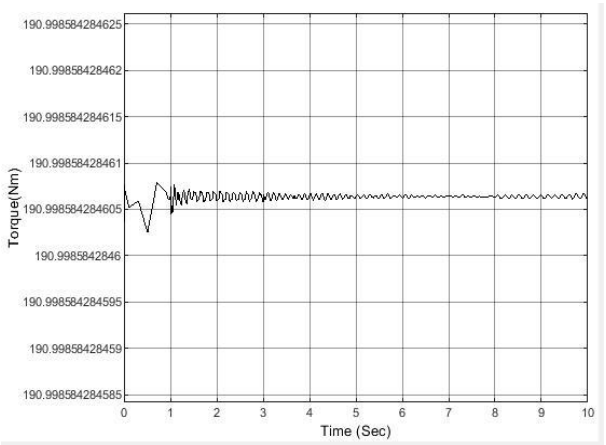

Fig. 8.Torque characteristics of the high-speed train motor

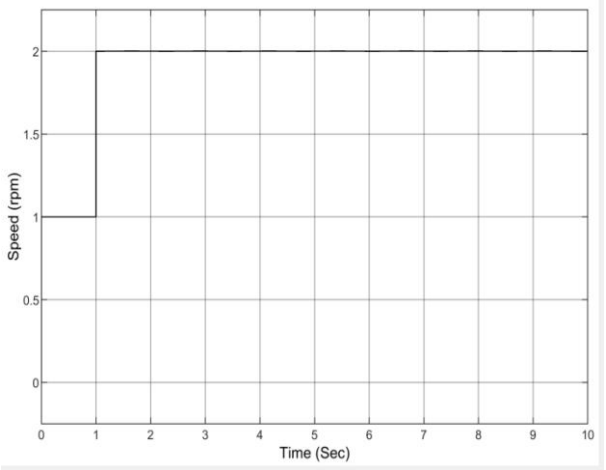

Fig. 9.Output graphic representation of the speed of the motor

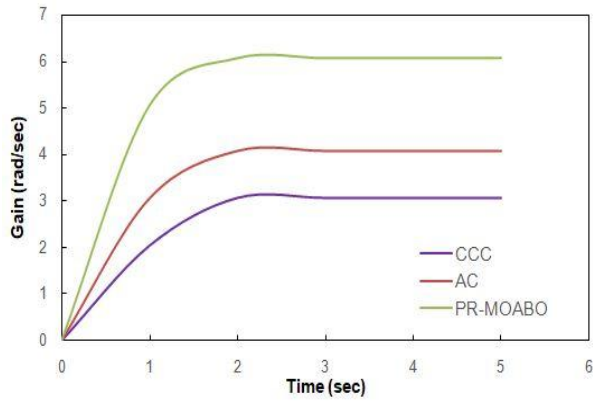

Fig. 10. Comparison of proposed gain (rad/sec) with the existing methods

The existing methodology used adaptive controller evaluated the health system of the train also cooperative cruise controller is utilized for communication purposes in railway, which means the cooperative cruise control is designed for multiple trains for message transformation purposes in Fig. 10. Besides these, while implementing the cruise controller with BLDC motor in high-speed trains, the gain value is obtained as 3.08 rad/sec. Thus the gain achieved by the adaptive and cruise controller is elaborated in Table I.

Moreover, the speed control of the high-speed train proposed braking system compared with the other existing controller, which is illustrated in Fig. 11.

Table- I: Comparison of proposed gain with existing methods

Time (sec)	Cooperative Cruise Control	Adaptive controller	PR-MOABO
1	2.05	3.05	5.05
2	3.08	4.07	6.07
3	3.08	4.07	6.07
4	3.08	4.07	6.07
5	3.08 [a]	4.07 [b]	6.07 [c]

[a] the gain constant values used in the cooperative cruise control at the time 5sec.
[b] the gain constant values used in the adaptive controller at the time 5sec.
[c] the gain constant values used in the proposed controller with optimization at the instant 5sec.

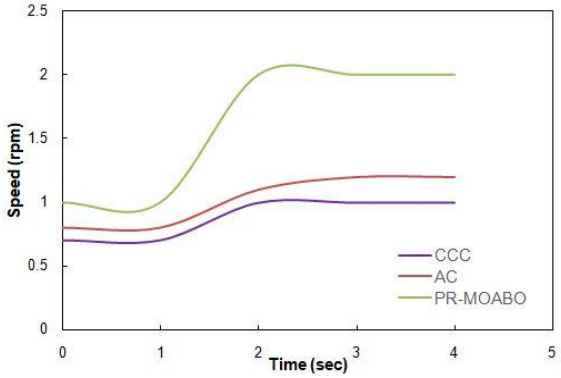

Fig. 11. Comparison of speed control of motor in high-speed train with existing techniques

While the PR controller gain is increased at the same time the speed of the BLDC motor also gets increased. Thus the usage of PR controller in BLDC motor can enhance the performance of the motor. Thus the train can process or run in high speed. Consequently, the enhanced braking system with optimization approach of control at high-speed trains. Hence the proposed system can reduce train accidents. Moreover, the torque value measure achieved by cruise controller, adaptive controller, and propose PR controller with BLDC motor are defined in Table II.

The lower revolving speed in BLDC motor can achieve less shear strength and high frictional resistance. The error is raised between the reference signal and the control signal. Besides, the PR controller achieved less error percentage, which is compared with the conventional controllers in Fig. 12. From this, the combination of MOABO with PR controller validated tremendously the error percentage minimization.

Table- II: Comparison of proposed braking system with existing methods

Time (sec)	Cooperative Cruise Control	Adaptive controller	PR-MOABO
0	0.7	0.8	1
1	0.7	0.8	1
2	1	1.1	2
3	1	1.2	2
4	1 [a]	1.2 [b]	2 [c]

[a] the maximum torque obtained by the cooperative cruise control is 1n-m at the 4 sec instant.
[b] the maximum torque attained by the adaptive control is 1.2 n-m at the 4 sec instant.
[c] the maximum torque obtained by the proposed controller with optimization is 2 n-m at the 4 sec instant.

Table- III: Comparison of Error Percentage

Controller	Cooperative Cruise Control	Adaptive controller	PR controller with MOABO
Error percentage [a]	0.3	0.24	0.1826

[a] error percentage is defined as (|true value-simulated value|\true value) x100%.

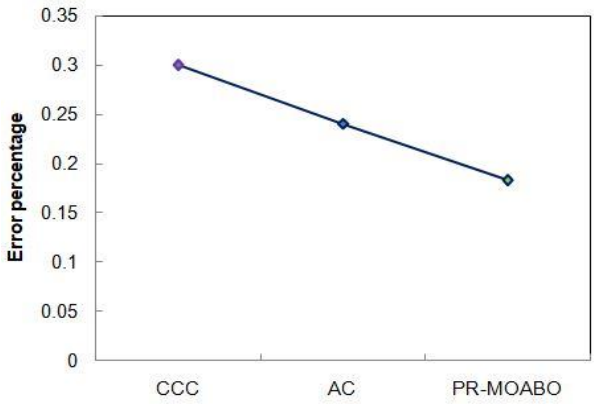

Fig. 12. Comparison of speed control of motor in high-speed train with existing techniques

Therefore, the implementation result shows the error percentage of both adaptive and cruise controller. From this, the result shows that the PR controller can have less error rate and high efficiency. However, the PR controller has less error rate compared to the conventional controller, also while the usage of optimization strategy can enhance the performance of PR controller because it optimized the error which the PR controller has obtained. Thus finally the PR controller achieved a very low error rate, and the comparison results ranges are detailed in Table III.

This shows the efficiency of the proposed approach of the braking system in a high-speed train.

V. CONCLUSION

The aim of this research is replacing the novel electric regenerative braking system instead of a friction mechanism. Therefore this elaborated the control based electric braking scheme in a high-speed train, thus the current controlled the brake pads and friction. A novel PR with MOABO controller was designed in high-speed train braking system and achieved high gain. Moreover, the stability of the proposed controller in the braking system is validated by the Lyapunov function and satisfied the conditions under different operating conditions. Consequently, the simulation outcomes are validated and attained the gain of PR controller by MOABO tuning to the braking system as 479.6 rad /sec. In addition, the proposed controller with an optimization mechanism optimized the percentage of error rate at 0.1826%. Thus the proposed system is improved the braking system in high-speed trains to avoid the train accident consequently reducing the wear rate and so on.

REFERENCES

1. J. Campos, G. D. Rus, "Some stylized facts about high-speed rail: A review of HSR experiences around the world," *Transport policy*, Vol. 16, Issue 1, 2009, 19–28. https://doi.org/10.1016/j.tranpol.2009.02.008
2. M. Kyriakidis, R. Hirsch, A. Majumdar, "Metro railway safety: An analysis of accident precursors," *Safety science*, Vol. 50, Issue 7, 2012, 1535–1548. https://doi.org/10.1016/j.ssci.2012.03.004
3. E. K. Liebemann, K. Meder, J. Schuh, G. Nenninger, "Safety and performance enhancement: The Bosch electronic stability control (ESP)," *SAE Technical Paper*, 2004.
4. T. Moreno, V. Martins, C. Reche, M. C. Minguillon, "Air quality in subway systems," *Non-Exhaust Emissions*, 2018, pp. 289–321. https://doi.org/10.1016/B978-0-12-811770-5.00013-3
5. X. Xiao, Y. Yin, J. Bao, L. Lu, "Review on the friction and wear of brake materials," *Adv. Mech. Eng.*, Vol. 8, Issue 5, 2016. https://doi.org/10.1177/1687814016647300
6. B. Zornoza, C. Tellez, J. Coronas, J. Gascon, "Metal organic framework based mixed matrix membranes: An increasingly important field of research with a large application potential," *Microporous and Mesoporous Materials*, Vol. 166, 2013, 67–78. https://doi.org/10.1016/j.micromeso.2012.03.012
7. K. S. Munir, P. Kingshott, C. Wen, "Carbon nanotube reinforced titanium metal matrix composites prepared by powder metallurgy-a review," *Crit. Rev. Solid State and Mater. Sci.*, Vol. 40, Issue 1, 2015, 38–55. https://doi.org/10.1080/10408436.2014.929521
8. T. Peng, Q. Yan, G. Li, X. Zhang, Z. Wen, X. Jin, "The braking behaviors of Cu-based metallic brake pad for high-speed train under different initial braking speed," *Tribol. Lett.*, Vol. 65, Issue 4, 2017, 135. https://doi.org/10.1007/s11249-017-0914-9
9. H. Harrison, T. Mccanney, J. Cotter, "Recent developments in coefficient of friction measurements at the rail/wheel interface," *Wear*, Vol. 253, Issue 1-2, 2002, 114–123. https://doi.org/10.1016/S0043-1648(02)00090-X
10. R. G. Du Toit, D. H. Diamond, P. S. Heyns, "A stochastic hybrid blade tip timing approach for the identification and classification of turbomachine blade damage," *Mech. Syst. Signal Pr.*, Vol. 121, 2019, 389-411. https://doi.org/10.1016/j.ymssp.2018.11.032
11. S. Xie, Z. Chen, L. Wang, T. Takagi, "An inversion scheme for sizing of wall thinning defects from pulsed eddy current testing signals," *Int. J. Appl. Electromagnetic Mech.*, Vol. 39, Issue 1-4, 2012, 203–211. DOI: 10.3233/JAE-2012-1462
12. S. E. Gay, M. Ehsani, "Parametric analysis of eddy-current brake performance by 3-D finite-element analysis," *IEEE Trans. Magn.*, Vol. 42, Issue 2, 2006, 319–328. DOI: 10.1109/TMAG.2005.860782
13. E. J. Park, D. Stoikov, L. F. da Luz, A. Suleman, "A performance evaluation of an automotive magnetorheological brake design with a sliding mode controller," *Mechatronics*, Vol. 16, Issue 7, 2006, 405–416. https://doi.org/10.1088/0957-0233/19/12/122001
14. C. C. Ciang, J. R. Lee, H. J. Bang, "Structural health monitoring for a wind turbine system: a review of damage detection methods," *Meas. Sci. Technol.*, Vol. 19, Issue 12, 2008, 122001. https://doi.org/10.1088/0957-0233/19/12/122001
15. X. Xu, J. Peng, R. Zhang, B. Chen, F. Zhou, "Adaptive Model Predictive Control for Cruise Control of High-Speed Trains with Time-Varying Parameters," *J. Adv. Transport.*, 2019.
16. I. Serrano-Munoz, J. Rapontchombo, V. Magnier, "Evolution in microstructure and compression behaviour of a metallic sintered friction material after braking," *Wear*, 2019, p. 202947. https://doi.org/10.1016/j.wear.2019.202947
17. P. Zhang, L Zhang, K. Fu, P. Wu, J. Cao, C. Shijia, "The effect of Al2O3 fiber additive on braking performance of copper-based brake pads utilized in high-speed railway train," *Tribol. Int.*, Vol. 135, 2019, 444–456. https://doi.org/10.1016/j.triboint.2019.03.034
18. P. Zhang, L. Zhang, K. Fu, P. Wu, J. Cao, C. Shijia, X. Qu, "Fade behaviour of copper-based brake pad during cyclic emergency braking at high-speed and overload condition," *Wear*, Vol. 428, 2019, 10–23. https://doi.org/10.1016/j.wear.2019.01.126
19. Y. Xiao, Z. Zhang, P. Yao, K. Fan, H. Zhou, T. Gong, "Mechanical and tribological behaviors of copper metal matrix composites for brake pads used in high-speed trains," *Tribol. Int.*, Vol. 119, 2018, 585–592. https://doi.org/10.1016/j.triboint.2017.11.038
20. P. Zhang, L. Zhang, K. Fu, J. Cao, C. Shijia, X. Qu, "Effects of different forms of Fe powder additives on the simulated braking performance of Cu-based friction materials for high-speed railway trains," *Wear*, Vol. 414, 2018, 317–326. https://doi.org/10.1016/j.wear.2018.09.006
21. A. Khazaee, H. A. Zarchi, G. R. A. Markadeh, "Real-Time Maximum Torque per Ampere Control of Brushless DC Motor Drive with Minimum Torque Ripple," *IEEE Trans. Power Electron.*, 2019. DOI: 10.1109/TPEL.2019.2918711
22. Y. J. Liu, S. Lu, S. Tong, X. Chen, C. L. P. Chen, D. J. Li, "Adaptive control-based barrier Lyapunov functions for a class of stochastic nonlinear systems with full state constraints," *Automatica*, Vol. 87, 2018, 83–93. https://doi.org/10.1016/j.automatica.2017.07.028
23. Y. Li, D. Zhao, Y. Q. Chen, I. Podlubny, C. Zhang, "Finite Energy Lyapunov Function Candidate for Fractional Order General Nonlinear Systems," *Communications in Nonlinear Sci. Numer. Simul.*, 2019, p. 104886. https://doi.org/10.1016/j.cnsns.2019.104886
24. Z. Wu, F. Albalawi, Z. Zhang, J. Zhang, H. Durand, "Control Lyapunov-Barrier function-based model predictive control of nonlinear systems," *Automatica*, Vol. 109, 2019, 108508. https://doi.org/10.1016/j.automatica.2019.108508
25. S. Liu, B. Jiang, Z. Mao, S. X. Ding, "Adaptive Backstepping Based Fault-tolerant Control for High-speed Trains with Actuator Faults," *Int. J. Control Autom. Syst.*, Vol. 17, Issue 6, 2019, 1408–1420. https://doi.org/10.1007/s12555-018-0703-8
26. W. Bai, Z. Lin, H. Dong, B. Ning, "Distributed Cooperative Cruise Control of Multiple High-Speed Trains Under a State-Dependent Information Transmission Topology," *IEEE Trans. Intell. Transp. Syst.*, 2019. DOI: 10.1109/TITS.2019.2893583

AUTHOR PROFILE

Saranu Ravikumar is working as an Assistant Professor in the Department of Mechanical Engineering from Bapatla Engineering College, Bapatla, Andhra Pradesh, India. He received his Master of Technology in Industrial Tribology, Machine Dynamics and maintenance engineering from Indian Institute of Technology, Delhi in 2009 and Bachelor of Technology in Industrial and production engineering from R. V. R & J. C College of Engineering, Guntur, Andhra Pradesh. His Master project on Bearing fault identification using vibration and sound monitoring. He presented his master project paper in IUTAM symposium on emerging trends in rotor dynamics, 23-26 March 2009. At present he is doing his Ph. D (part time) on Metal matrix composites in Andhra University, Visakhapatnam. He has teaching experience of more than 10 years in the area of Mechanical Engineering.